Study on the effect of low-temperature atmospheric pressure plasma jet on the morphofunctional properties of living tissues (in vivo)

© *K.M. Giraev*[1,2], *N.A. Ashurbekov*[1], *E.Kh. Israpov*[1,2], *G.Sh. Shakhsinov*[1], *V.R. Abdulaev*[1], *K.M. Rabadanov*[1], *Z.M. Isaeva*[1]

[1] Dagestan State University,
367000 Makhachkala, Dagestan Republic, Russia
[2] Amirkhanov Institute of Physics, Dagestan Federal Research Center, Russian Academy of Sciences,
367030 Makhachkala, Dagestan Republic, Russia

e-mail: kamal_giraev@mail.ru, nashurb@mail.ru

The results of spectral-fluorescent and diffuse-optical studies of living tissues under the effect of low-temperature atmospheric pressure plasma jet in a mixture of air and argon are presented. Potential fluorophores are identified and coefficients of optical absorption and transport scattering of tissues are determined. It was revealed plasma jet irradiation of tissue leads to an increase in the intensity of fluorescence and the diffuse reflection coefficient, which is linked with a twofold increase in the transport scattering coefficient and a change in the concentration of endogenous chromophores — a reducing water content, lipids and bilirubin to 20%, and an increasing levels of oxygen saturation to 10%. On the basis of the analysis, it is shown that the therapeutic effect of low-temperature plasma can be associated with increased antioxidant protection and the development of compensatory dehydration processes.

Keywords: biological tissues, cold plasma, probing, spectroscopy, fluorescence, diffuse reflection, optical coefficients, light scattering, biochemistry, morphology.

DOI: 10.21883/EOS.2022.05.54452.2697-21

1. Introduction

One of the promising and rapidly developing areas of the radiation medicine for the recent time is plasma medicine demonstrating a high therapeutic efficiency in dermatology, cosmetology, stomatology, etc. (e.g., [1–4]). At the same time, qualitative nature of the results of research and the absence of details on physical, chemical and biological processes of interaction of low-temperature plasma with the tissues of visceral organs are the reasons for a high relevance of this scientific problem.

Physical and chemical features of interaction of plasma radiation with biological objects have a unique nature, as a consequence of complex composition and mechanisms of elementary processes in plasma, as well as variety of the structure of biological tissues and cells. The known factors of such effect can include electromagnetic fields and UV radiation, charged particles, oxygen containing (O, O_{2-}, O_3, H_2O_2) and nitrogen containing radicals (N, NO, NO_2, NO_3, N_2O_5) [5–9].

The foregoing leads not only to selective effect of plasma for biological objects of different level of metabolism (from bactericide effect to induction of complex biochemical reactions), but also to a synergetic effect. In the complex, these effects form the ground for curing pathologies, such as erosive and ulcerative lesions, virus and mycotic infections, etc. [1–12]. However, regardless of a high potential of the plasma therapy, there is a series of issues to resolve. In particular, we need to better understand the biochemical mechanisms of selective effect of the low-temperature plasma both for atypical tissues containing malignant cells, and for the adjacent normal biological tissues.

Important information on the structure, physiological and biochemical condition of a biological object can be provided by the method of combined laser-induced fluorescent (LIF) spectroscopy and diffusion reflectometry. Such approach is based on serial measurement and analysis of the spectra of fluorescence and coefficient of diffusion reflection and is low invasive, technically simple and informative method of life-time diagnostics of many pathologies, including malignant transformation processes [13–20]. Application of this method for the tasks of development of plasma therapy would allow to reveal the dynamics of quantitative characteristics of physical, chemical and biological processes, thus evaluating the degree and the system of monitoring of the efficiency of low-temperature plasma treatment of biological objects *in situ*.

The purpose of the work is to study the dynamics of structural and morphological, physiological and biochemical properties of biological tissues in vivo under effect of low-temperature plasma jet at atmospheric pressure by using the methods of optical spectrometry. At that, the following tasks were solved:

— LIF spectra were measured and potential groups of endogenic fluorophores were determined;

— spectra of the coefficient of diffusion reflection were measured and the coefficients of absorption and transport scattering for intact and irradiated biological tissues within the range of wavelengths 250−1500 nm were determined.

Based on the results of spectral studies, the most important physical and biochemical parameters were identified and possible mechanisms of interaction of the low-temperature plasma with biological objects are discussed.

2. Materials and methods

Materials of the study

Spectral and optical studies of biological tissues under effect of low-temperature plasma jet at atmospheric pressure were performed on the tissues of liver *in vivo* of 20 mature males of white Wistar rats approximately of the same age and weight (250 ± 30 g). 24 hours before the experiment beginning, rats were weighed and kept for 24 hours with no water and food in order to preserve the body general biochemical background. Immediately before experimental studies, abdominal cavity of rats was dissected, while under general narcosis, and hepatic lobes were carefully exposed in the injury. For the sake of minimization of distortions introduced by physiological factors (breathing, muscle spasms of a biological object, etc.) into the experiment, the organ under study was immobilized on a stand, placed over the rat body.

All applicable international and institutional principles of care and use of animals were observed.

Experimental scheme

The general scheme of the experiment was to measure the spectra of fluorescence $F(\lambda)$ and diffusion reflection $R_d(\lambda)$ of liver tissues *in vivo* before and after plasma probing. Meanwhile, only uniform sites of liver tissue undergone treatment and studies, whose area was fixed by putting a mask onto biological tissue with a window having diameter of about 5.0 mm.

Plasma irradiation of biological tissues was done by scanning them with plasma radiation during about 5−7 min. Whereas, the samples were arranged in perpendicular to the torch at the distance of 3.0 cm from the end of plasma waveguide, and the flow of gas was recorded at the value of 0.32 l/min, at which the plasma torch has the highest length. Preliminary measurements had shown that the temperature of plasma jet did not increase over 2°C relative to the room temperature, which, in turn, allowed to exclude thermal effect for biological objects.

3 series of spectral measurements of $F(\lambda)$ and $R_d(\lambda)$ were performed for each sample of biological tissues. Final result on the studied samples was determined by averaging serial measurements based on the root-mean-square deviation

$\delta = \sqrt{\sum_{i=1}^{n}((\xi - \xi_i)^2/n(n-1)}$, where n — the number of the series of measurements, ξ_i — spectra of fluorescence and coefficient of diffusion reflection for the i-th series, ξ — the average value of intensity of fluorescence and reflection for biological tissues at each spectral point, determined as $\sum_{i=1}^{n} \xi_i/n$. Therefore, each of the spectral data on $F(\lambda)$ and $R_d(\lambda)$ given in the work refer to an averaged value of the statistical material selected and systematized for intact and irradiated biological tissues.

Source of plasma radiation

Barrier discharge in a cylindrical plasma waveguide was used to create the source of low-temperature plasma radiation, wherein argon in presence of the atmospheric pressure air is passed through the discharge gap. The plasma source (Fig. 1, *a*) was an electrode system (*1*) of the needle−ring type, wherein tungsten wire (diameter of 0.5 mm) was placed inside quartz tube (*2*) (inner diameter — 1.0 mm, outer diameter — 7.0 mm) and used as a high-voltage electrode. Grounded copper ring with the width of 10 mm was put onto quartz tube at the distance of 60 mm from it. A mixture of pure argon (99.999%) was used as the working gas, and the gas flow was controlled by means of the GE50A flow meter (MKS Instruments, USA).

A high-voltage nano-second transformer-type generator working in the frequency-periodic mode, with the voltage aperiodic pulses repetition frequency of 10–100 Hz, was used for plasma jet formation (*3*). Amplitude of positive semiwave of the voltage pulse was controlled within the range of 8–12 kV at the pulse rise time of ~ 50 ns. At that, the discharge current was controlled by means of the Model 4100 current transformer (Pearson electronics, USA), and electrical signals were recorded by means of the TDS2024B oscillograph (Tektronix, USA).

Spectral characteristics of the low-temperature plasma, as well as the image of the plasma torch itself and its 3D projection are shown in Fig. 1, *b* and *c*, accordingly.

Spectral optical measurements

Measurement of spectra of fluorescence $F(\lambda)$ and coefficient of diffusion reflection $R_d(\lambda)$ was performed on a laser-spectrometer complex with the standard scheme, by using fiber-optic system (Fig. 1, *a*). Excitation of fluorescence spectra was performed by radiation from the LP603 optical parametric generator equipped with LQ529 pumping laser (*4*) (Solar LS, Belorussia) at the wavelengths 355 and 410 nm, and of the spectra of diffusion reflection coefficient — by radiation from deuterium/halogem lamp AvaLight-DH-S-BAL (*5*) (Avantes, the Netherlands).

Y-shaped measuring probe, consisting of two „hoses" (transmission (*6*) and receiver (*7*)) and a contact catheter (*8*), wherein lightguide channels were coaxially arranged (fiber diameter 200 μm, numerical aperture 0.22), was used as a fiber-optic system. Fiber lightguides forming the central channel of the probe (7 fibers — for excitation
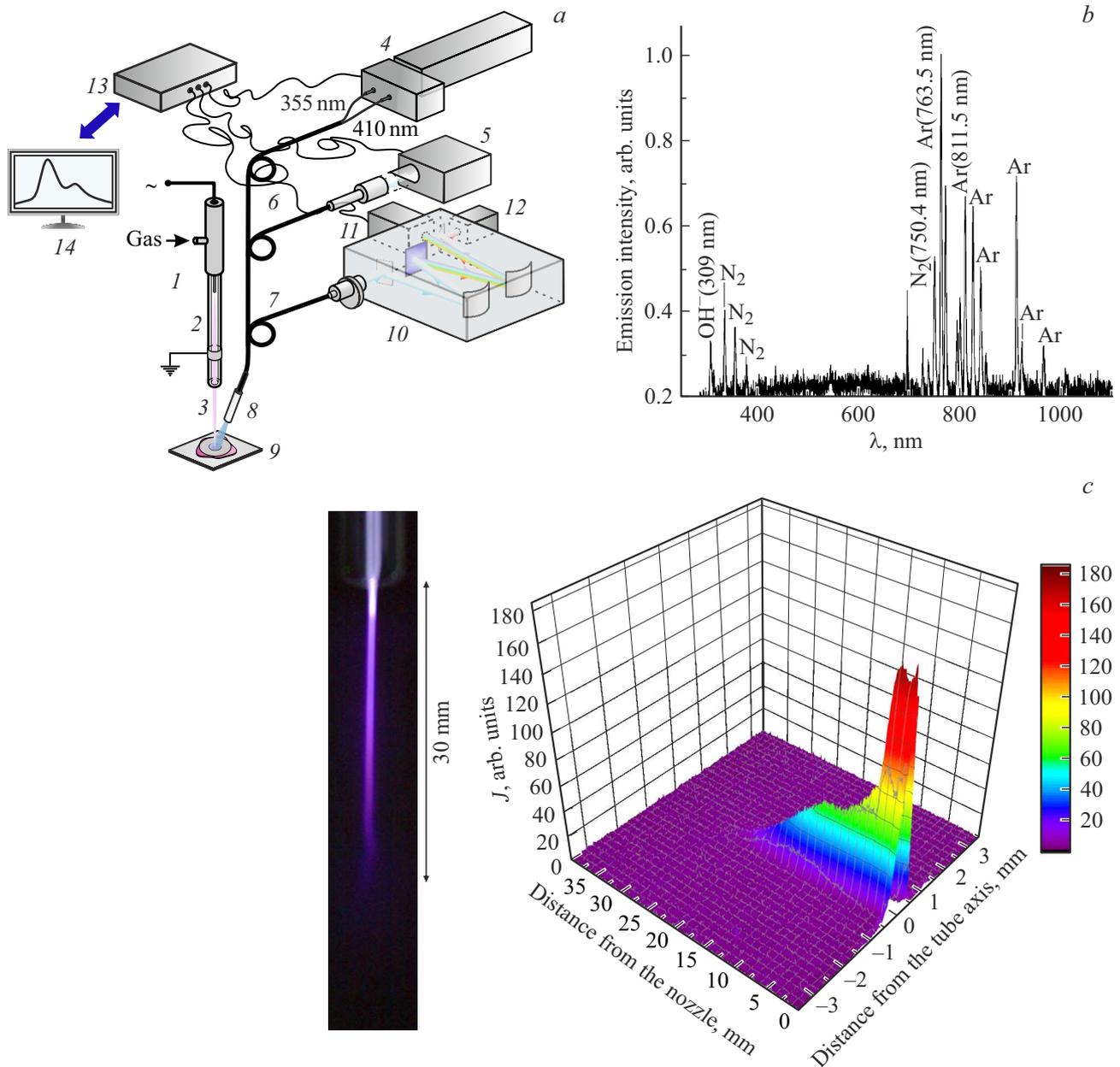
Figure 1. (*a*) Experimental unit block diagram: *1* — source of low-temperature plasma radiation; *2* — quartz tube with needle−ring electrode system; *3* — plasma torch; *4* — optical parametrical generator equipped with a pumping laser; *5* — deuterium/halogen lamp; *6* — transmission „hose" of fiber-optic probe; *7* — receiver „hose"; *8* — contact catheter of the probe; *9* — biological tissue sample; *10* — monochromator/spectrograph; *11* — CCD-matrix camera; *12* — infrared detector; *13* — controller; *14* — PC. (*b*) Spectral characteristics of radiation of low-temperature plasma. (*c*) Image of plasma torch and its 3D projection.

of spectra of $R_d(\lambda)$ and 12 — for $F(\lambda)$) were intended for feeding the excitation radiation to biological tissue (*9*), and the peripheral lightguides (72 fibers) formed the registration channel and served for collection of response photosignals and their transmission to spectrograph. At that, the excitation regions of signals $R_d(\lambda)$ and $F(\lambda)$ coincided and had the diameter of about 2.0 ± 0.5 mm, and the registration area uniformly overlapped the excitation area, being about 2 times larger than the excitation spot.

Spectral analysis of photosignals was performed within spectral interval of $250-1500$ nm by means of automated two-channel monochromator/spectrometer MS3504i (*10*) (SOL-Instruments, Belorussia) interfaced with the CCD-camera HS-101(HR)-2048 × 122 (*11*) (Hamamatsu, Japan) and infrared detector IGADAT-010TE (*12*) (SOL-Instruments). Bethlehem locking light filters with the light transmission of 70% within the spectral range of $390-800$ nm and $450-1000$ nm were used for measurements of the fluorescence spectra, and normalization of the
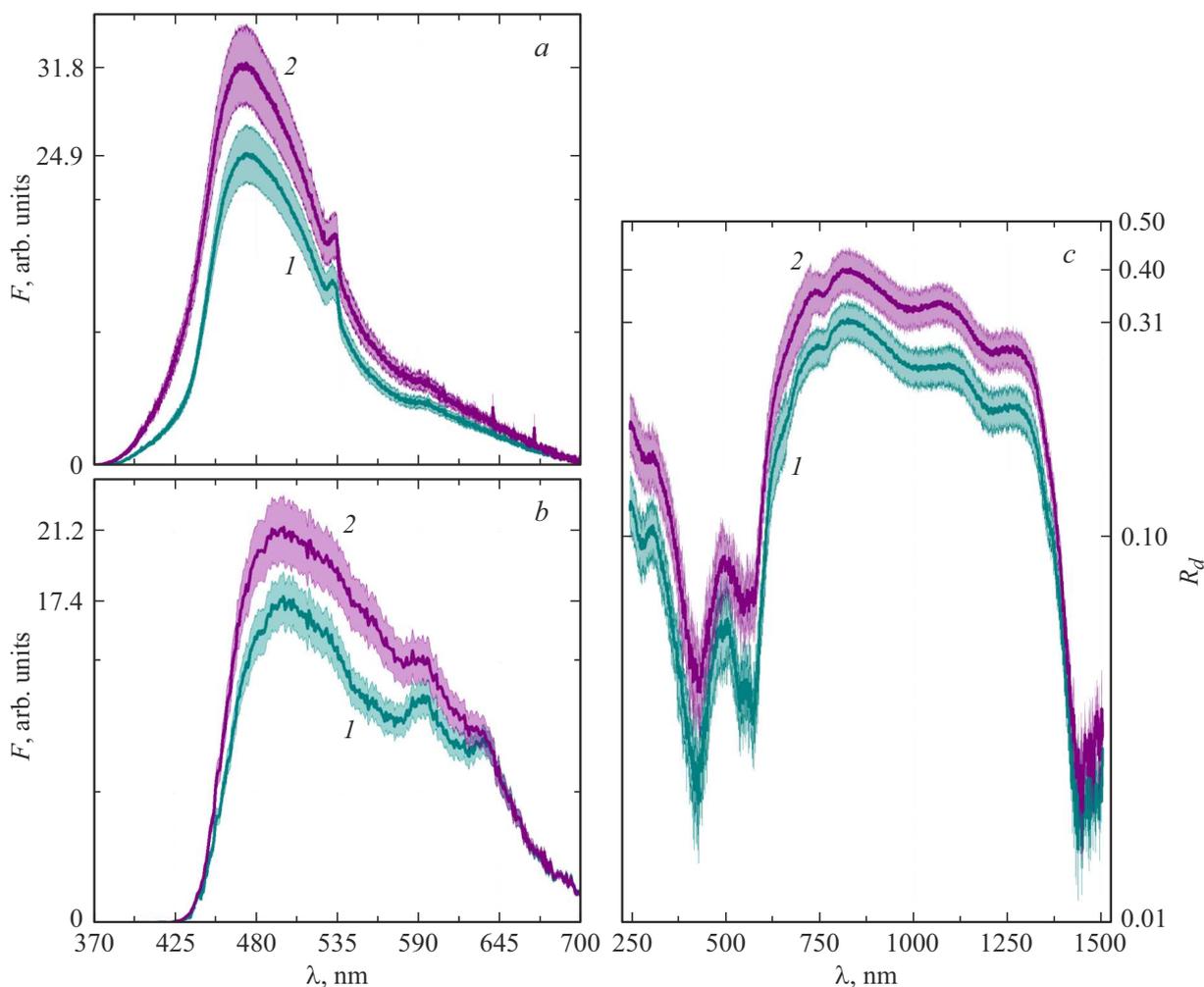
Figure 2. Spectra of laser-induced fluorescence $F(\lambda)$, obtained during excitation at the wavelengths of 355 (*a*) and 410 nm (*b*), as well as the spectra of the coefficient of diffusion reflection $R_d(\lambda)$ (*c*) for intact biological tissues (*1*) and biological tissues treated with plasma radiation with the duration of 7 min (*2*).

spectra of diffusion reflection was performed by means of the reference reflector WS-2 (Avantes, the Netherlands).

Optical properties determination procedure

For determination of spectral dependence of the coefficients of optical absorption $\mu_a(\lambda)$ and transport dissipation $\mu'_s(\lambda)$ for the studied biological tissues, we used in our work the inverse Monte-Carlo method (IMCM) in approximation of semi-infinite medium based on the spectral data of the diffusion reflection coefficient $R_d(\lambda)$. The algorithm of the used method in short refers to a serial implementation of the following steps.

1. Calculation of initial approximations of the parameters $\mu_a(\lambda)$ and $\mu'_s(\lambda)$ based on the experimental data $R_d^{\mathrm{Exp}}(\lambda)$, by using the ratio [21–23]:

$$R_d^{\mathrm{Exp}}(\lambda) = \exp\left\{ K\left[3\left(1 + \frac{\mu'_s(\lambda)}{\mu_a(\lambda)}\right)\right]^{-\frac{1}{2}}\right\}, \quad (1)$$

$$\mu_a(\lambda) = \mu_a^{\mathrm{chrom}}(\lambda) + \mu_a^{\mathrm{tissue}}(\lambda), \quad (2)$$

$$\mu_a^{\mathrm{chrom}}(\lambda) = V_{\mathrm{B}}\alpha\mu_a^{\mathrm{HbO}}(\lambda) + V_{\mathrm{B}}(1-\alpha)\mu_a^{\mathrm{Hb}}(\lambda)$$

$$+ V_{\mathrm{W}}\mu_a^{\mathrm{W}}(\lambda) + V_{\mathrm{Br}}\mu_a^{\mathrm{Br}}(\lambda) + V_{\mathrm{L}}\mu_a^{\mathrm{L}}(\lambda), \quad (3)$$

where $\mu_a(\lambda)$ and $\mu'_s(\lambda)$ are the spectra of absorption and transport dissipation coefficients for biological tissues *in vivo*, accordingly; K is the constant that depends on the refraction index of biological tissue; λ is the wavelength; $\mu_a^{\mathrm{chrom}}(\lambda)$ and $\mu_a^{\mathrm{tissue}}(\lambda)$ are the spectra of chromophores and biological tissue absorption coefficients *in vitro*; μ_a^{HbO}, $\mu_a^{\mathrm{Hb}}(\lambda)$, $\mu_a^{\mathrm{W}}(\lambda)$, $\mu_a^{\mathrm{Br}}(\lambda)$ and $\mu_a^{\mathrm{L}}(\lambda)$ are the spectra of absorption coefficients for oxyhemoglobin, deoxyhemoglobin, water, bilirubin and lipids, accordingly [21,24]; α — blood oxygenation degree of the studied area of biological tissue; V_{B}, V_{W}, V_{Br} and V_{L} — parameters describing volume ratio of blood, water, bilirubin and lipids in biological tissues, accordingly.

Spectral dependence of the indicator $\mu'_s(\lambda)$ can be approximated with a good accuracy by two-degree-of-freedom

function of the type [21–23]:

$$\mu'_s(\lambda) = A_M \lambda^{-B_M} + A_R \lambda^{-B_R}, \qquad (4)$$

where A_M and A_R — dimensionless parameters being the functions of concentration of dissipating particles (Mie and Rayleigh, accordingly) that form a total level of the coefficient μ'_s, meanwhile the wave exponents B_M and $B_R \to 4$ describe the average size of dissipating particles and determine the inclination angle of spectra of the coefficient μ'_s.

2. Determination of the calculation parameters of the coefficient of diffusion reflection $R_d^{\text{Calc}}(\lambda)$ based on the values of initial approximations of the coefficients $\mu_a(\lambda)$ and $\mu'_s(\lambda)$, by using the Monte-Carlo method.

3. Drawing the target function and its minimization: $F = \left(R_d^{\text{Exp}}(\lambda) - R_d^{\text{Calc}}(\lambda) \right)^2$.

4. Implementation of the minimization procedure based on the downhill simplex method [25] until the following condition is met:

$$\frac{|R_t^{\text{Exp}}(\lambda) - R_t^{\text{Calc}}(\lambda)|}{R_t^{\text{Exp}}(\lambda)} \le 0.1.$$

3. Results and discussion

Figure 2 shows typical spectra of laser-induced fluorescence $F(\lambda)$ (*a* and *b*) and of the coefficient of diffusion reflection $R_d(\lambda)$ (*c*) for intact tissue of liver (curve *1*) and during probing with cold plasma with exposure 7 min (curve *2*). As can be seen in figure, for the spectra of $F(\lambda)$ and $R_d(\lambda)$ of the studied biological tissues, there are both a series of common regularities, and specific features, which indicates the possibility of application of spectral optic methods in monitoring of the efficiency of plasma probing. In particular, during excitation at the wavelength of 355 nm (Fig. 2, *a*) the main maximum near to the wavelengths 472 ± 3 nm and two components at 532 ± 2 and 593 ± 10 nm is typical for the spectral contour of fluorescence $F_{355}(\lambda)$. The long wavelength components are more clearly identified in case of excitation of the spectra $F_{410}(\lambda)$ at the wavelength of 410 nm (Fig. 2, *b*), for which the maximum of intensity falls within the region of the wavelengths 500 ± 5 nm and illumination stripe near to 560 ± 5, 593 ± 3 and 635 ± 3 nm. At that, the presence of minima within the spectral interval of the wavelengths $400-440$ and $530-580$ nm, apparently, is caused by the presence of blood in biological tissues and the fluorescence photons reabsorption near to the hemoglobin absorption stripes. Wherein, the effect of plasma radiation in case of general increase of the intensity of spectra $F(\lambda)$ up to 1.5 times is accompanied both by the equalization of „dips" of spectral contour, and by attenuation of illumination at the wavelengths 532 ± 2, 593 ± 10 and 635 ± 3 nm by $20-25\%$.

For the spectra of the coefficient of diffusion reflection (Fig. 2, *c*) with inverse dissipation that determines the level of $R_d(\lambda)$, there are clear spectral stripes of absorption of blood (280 ± 5, 420 ± 3, 545 ± 3 and 575 ± 3 nm), lipids and water (760 ± 5, 990 ± 5, 1190 ± 5, 1450 ± 5 nm), near to which the spectrum of $R_d(\lambda)$ gets deep minima [21,24]. Typical values of the reflection coefficient, which are specific for intact tissues of liver, fall within the limits from 0.022 ± 0.05 in ultraviolet and near infrared regions to 0.31 ± 0.03 — for the therapeutic window area. At the same time, plasma-induced effects result in two times growth of intensity of reflection generally within the short wavelength region of the spectrum, meanwhile the increase of $R_d(\lambda)$ within the transparency window range does not exceed 30%.

The use of the root-mean-square deviation method as a statistical analysis of spectral data allowed to determine that the maximum spread of values of $F(\lambda)$ and $R_d(\lambda)$ did not exceed $10-15\%$ for the whole spectral interval of the study, except for the region of the wavelengths of 350 and 420 nm, where the spread for $R_d(\lambda)$ reached $25-30\%$.

For the purpose of getting quantitative information on the dynamics of biochemical activity of endogenic fluorophores, we performed the contour analysis of the fluorescence spectra of the studied biological objects along with the plasma probing during the work. The spectral breakdown procedure referred to application of a combination of the Gaussian and Lorentz functions, and is described in detail in the work [26].

Figure 3 shows the results of breakdown of the fluorescence spectra of $F_{355}(\lambda)$ and $F_{410}(\lambda)$ for intact tissues of liver (*a* and *c*) and under effect of cold plasma (*b* and *d*). As can be seen in figure, the spectra of fluorescence of the studied biological tissues are formed by at least seven groups of fluorophores (corresponding to the curve numbers in figure). According to the data in [27–29], out of the total number of biologically active substances, which are the most typical ones for the liver tissues, the following can be distinguished from these seven groups.

∗ Group *2* — coenzymes NADH/NAD(P)H (a reduced form of nicotinamide-adenine dinucleotide (phosphate)) with the maximum of excitation/emission at the wavelengths $\lambda_{\text{ex}}/\lambda_{\text{em}} \sim (336, 351)/470 \pm 5$ nm.

∗ Group *3* — vitamin A, with the maximum $\lambda_{\text{ex}}/\lambda_{\text{em}} \sim (315, 380)/510 \pm 5$ nm.

∗ Group *4* — flavin groups derivatives (FAD — oxidized form of flavin adenine dinucleotide and FMN — flavin mononucleotide) with $\lambda_{\text{ex}}/\lambda_{\text{em}} \sim (380, 450)/525 \pm 10$ nm.

∗ Group *5* — lipids (lipofuscin, seroid), $\lambda_{\text{ex}}/\lambda_{\text{em}} \sim 340-395/550 \pm 5$ nm.

∗ The groups *6* and *7* are derivatives of endogenic porphyrines with the maximum of excitation/emission within the region of the wavelengths $\lambda_{\text{ex}}/\lambda_{\text{em}} \sim 380-450/590-690$ nm.

Wherein the group *1* corresponding to illumination of structural proteins — collagen and elastin (the maximum of $\lambda_{\text{ex}}/\lambda_{\text{em}} \sim 325/405 \pm 5$ nm) within the spectra $F_{355}(\lambda)$ and the group *2* of fluorophores within the spectra $F_{410}(\lambda)$ are heavily weakened by spectral characteristics of locking
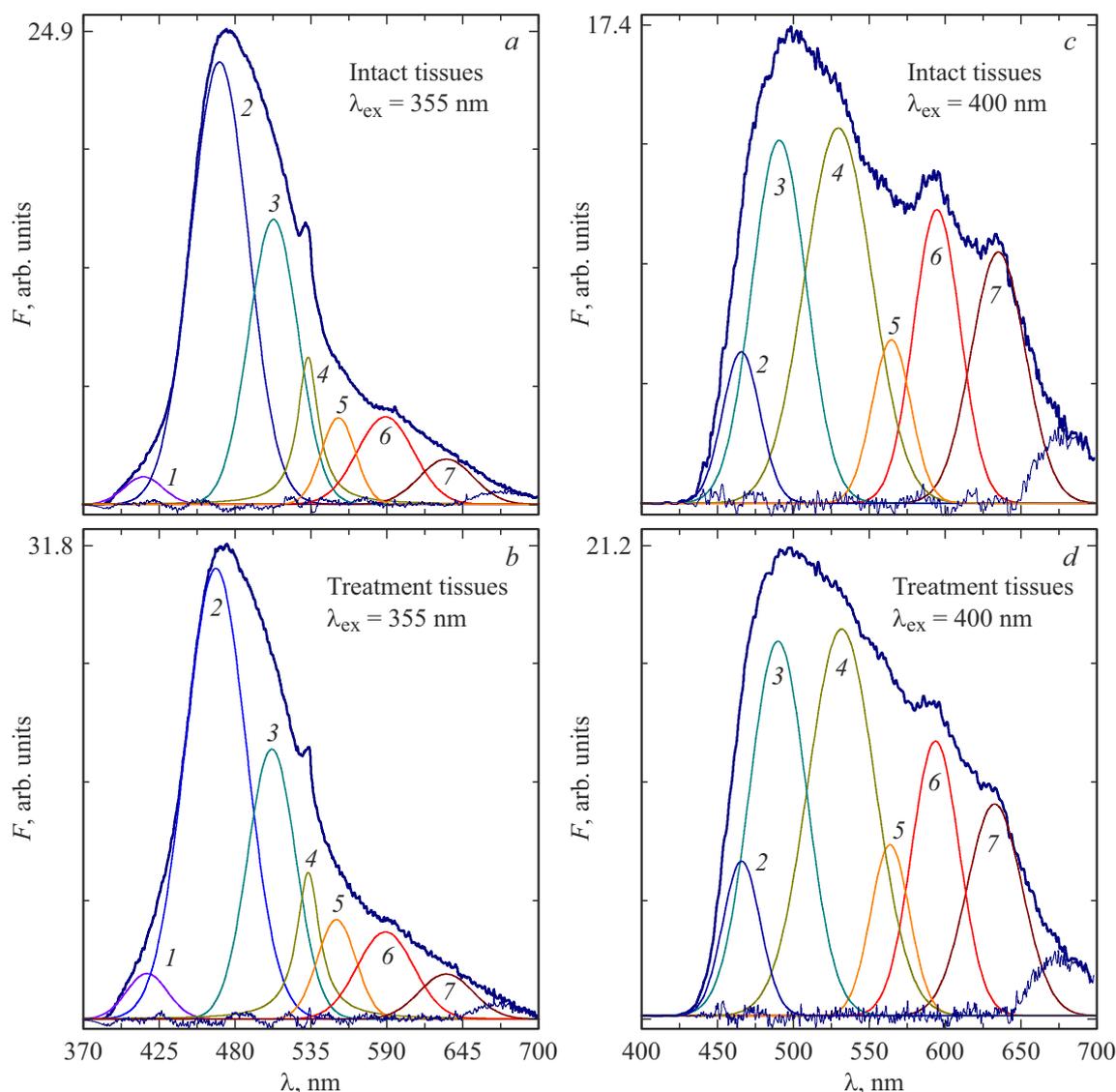
Figure 3. Contour analysis of the spectra of laser-induced fluorescence $F(\lambda)$ for intact tissues of liver (a, c) and under effect of low-temperature plasma with the exposure 7 min (b, d). The digits show spectral components of breakdown, corresponding to endogenic fluorophores.

light filters. For that reason, their role in further analysis of corresponding spectra of fluorescence was not considered.

Analysis of the results of spectral breakdown of $F(\lambda)$ indicates that in the process of plasma effect the most apparent changes are observed in the ratios and contributions of the *2*-nd and *4*-th groups. It is known that NADH molecules and the group of flavin derivatives are concentrated generally in mitochondria of hepatocytes and function as coenzymes of dehydrogenases in oxidation and reduction reactions, acting as a substrata electrons acceptor. While reducing, the chromophore NAD$^+$ accumulates positively charged ions of hydrogen H$^+$ and gets a bright fluorescence with a small shift towards the short wavelength region of the spectrum, at the same time, having catalyzed the reduction of flavin coenzyme FAD. Because of that, any changes in cellular metabolism affect the concentration of oxidized and reduced forms of these fluorophores and can be detected in the dynamics of ratios of their spectral components.

Based on the methodology of quantitative evaluation of the respiratory activity of mitochondria [29–31], the work evaluated the degree of the energy exchange of biological tissues by normalization of the intensity of illumination of flavin groups — F_{FAD} to the intensity of illumination of NAD(P)H — $F_{(NAD(P)H}$, as the ratio of areas under the curves of breakdown components — $S_{ex/em}$:

$$\kappa_1 = \frac{S^4_{355/530}}{S^4_{355/530} + S^2_{355/470}} = \frac{F_{FAD}}{F_{FAD} + F_{NAD(P)H}}.$$

Availability of information on other components of the fluorescence spectra breakdown enables introduction into the analysis of a series of additional values of the biological
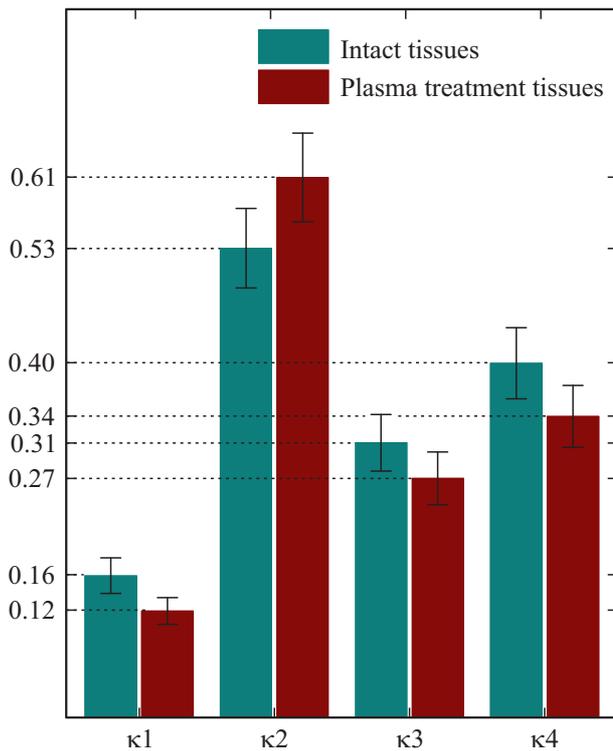
Figure 4. The diagram of spectral indices $\kappa_1 - \kappa_4$, describing the dynamics of contributions of endogenic fluorophores into total spectra of fluorescence of the liver tissues when probing by cold plasma radiation with the exposure of 7 min.

tissues functioning, which, similarly to the index κ_1 can be determined as

$$\kappa_2 = \frac{(S^3_{355/510} + S^3_{410/510})/2}{(S^3_{355/510} + S^3_{410/510}/2 + (S^4_{355/530} + S^4_{410/530})/2}$$

$$= \frac{F_{Vit\_A}}{F_{Vit\_A} + F_{FAD}},$$

$$\kappa_3 = \frac{(S^5_{355/560} + S^5_{410/560})/2}{(S^5_{355/560} + S^5_{410/560}/2 + (S^4_{355/530} + S^4_{410/530})/2)}$$

$$= \frac{F_{\text{Lipids}}}{F_{\text{Lipids}} + F_{\text{FAD}}},$$

$$\kappa_4 = \frac{(S^6_{355/595} + S^6_{355/635} + S^6_{410/595} + S^6_{(410/635}/4}{(S^6_{355/595} + S^6_{355/635} + S^6_{410/595} + S^6_{(410/635})/4+ \atop + (S^4_{355/530} + S^4_{410/530})/2}$$

$$= \frac{F_{\text{Porph}}}{F_{\text{Porph}} + F_{\text{FAD}}},$$

where κ_2 is the antioxidant index, κ_3 is the intracellular organs degradation index, and κ_4 is the hemoproteins degradation index.

Systematized data of the indices $\kappa_1 - \kappa_4$ for intact tissues of liver and under effect of plasma radiation (CAP) with the exposure of 7 min are given in Fig. 4. As can be seen

in figure, plasma treatment of biological tissues leads to decrease of the index of respiratory activity κ_1 down to 20%. Since the index κ_1 is caused by fluorescence of pyridine and flavin nucleotides, which are present mainly in mitochondria of hepatocytes, then its observed dynamics is caused by decrease of concentration of oxidized flavin derivatives and the increase of NADH concentration. This statement is also backed by the fact that the ratio NADH/NAD$^+$ in mitochondria is two orders higher versus their content in cytoplasm. In the aggregate with the obtained physiological data (the degree of blood filling and oxygenation of biological tissues) one may state also that NADH accumulation in mitochondria under the effect of plasma is not related with the conditions of hypoxia and activation of anaerobic glycolysis, and the index of respiratory activity κ_1 that reflects redox state of liver mitochondria, is caused by the dynamics of the complexes I and II of the respiratory chain [29–31].

Moreover, it is well known that activation of electrons transfer in the respiratory chain of mitochondria may be accompanied by amplification of the free radical generation, who have both positive, and negative effect, related with degradation of macromolecules and cellular structures. Unlike other organs, liver has a powerful antioxidant system (enzymatic and non-enzymatic) that blocks the process of oxidation and neutralizes the activity of free radicals. Wherein, key antioxidants are lipid soluble vitamins — vitamin A localized mainly in the membrane structures of hepatocytes and ensuring protection of lipid-protein matrix [29,32]. In this regard, the growth of the index of antioxidant protection κ_2 by 15% for the probed biological tissues indicates the increase of retinoids concentration in the medium. Since vitamin A is an exogenic antioxidant, then the detected amplification of illumination is related with its mobilization from blood and deposition in hepatocytes. This, in turn, allows to discuss the nature of therapeutic effect of cold plasma via amplification of antioxidant protection.

This assumption is confirmed by the dynamics of the indices of degradation of intracellular organs κ_3 and hemoproteins κ_4, caused by decrease of concentration of lipofuscin and porphyrines down to 30%. It is known that these substances are formed under the effect of active forms of oxygen as a result of free radical oxidation of cellular lipids and residues of proteins, and these are mainly originated from incomplete degradation of damaged mitochondria [29,33,34]. Therefore, the observed changes of the indices κ_3 and κ_4 also indicate favorable effect of plasma radiation for cellular structures, hepatocytes and liver tissue in general.

Analysis of the coefficient of diffusion reflection $R_d(\lambda)$, by using the inverse Monte-Carlo method, allowed to determine the dynamics of optical and spectral properties of biological tissues as far as cold plasma is acting. Figure 5 shows the spectra of the coefficients of optical absorption $\mu_a(\lambda)$ and transport dissipation $\mu'_s(\lambda)$, as well as their reconstruction into the spectra of the coefficient of reflection
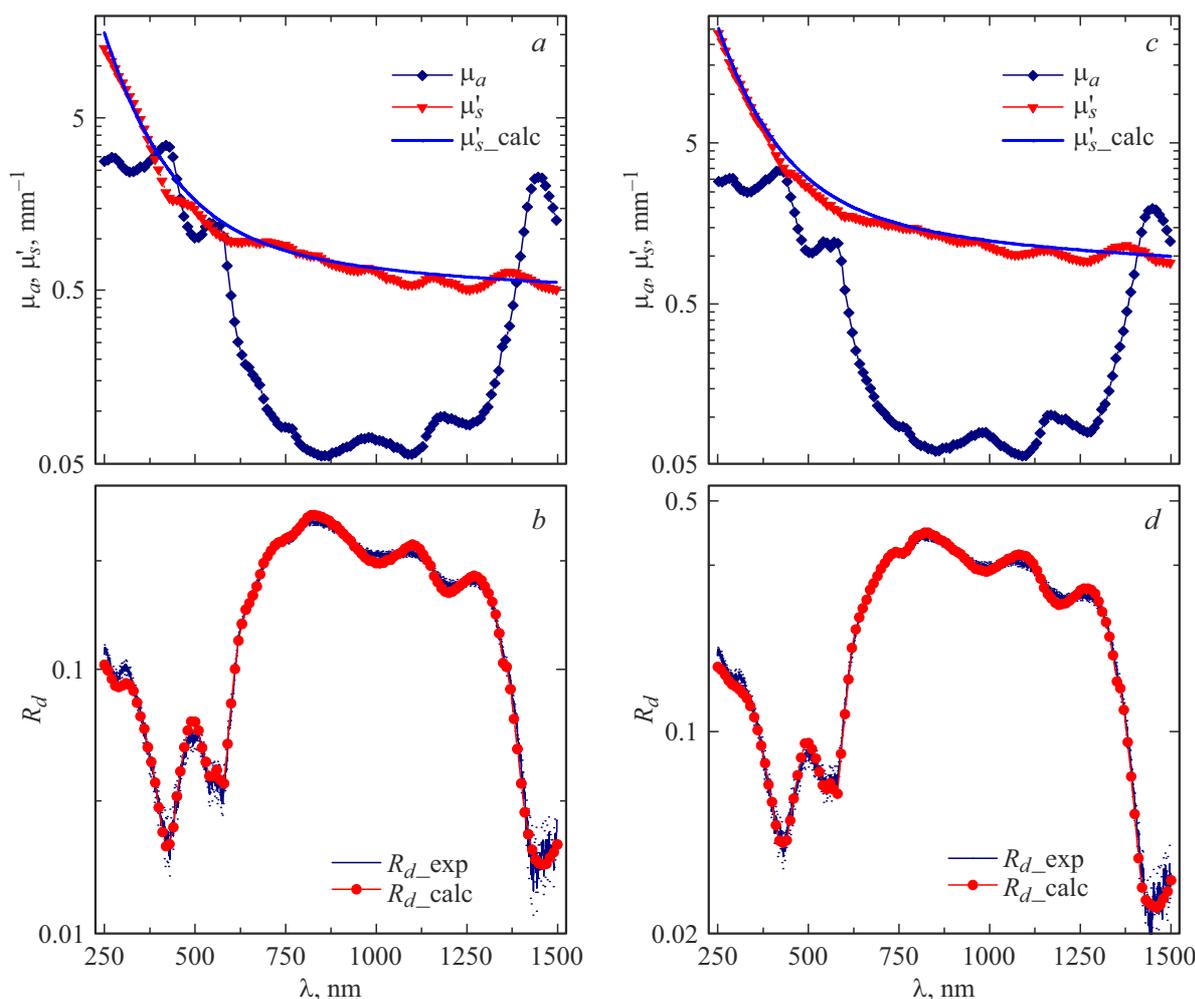
Figure 5. The spectra of coefficients of optical absorption $\mu_a(\lambda)$ and transport dissipation $\mu_s'(\lambda)$, as well as the spectra of coefficient of diffusion reflection $R_d(\lambda)$ and its reconstruction R_{d-}Calc for liver tissues before (a, b) and after exposure to cold plasma radiation (c, d). Continuous curve is the approximation of the coefficient of transport dissipation $\mu_s'{}_{-}$Calc.

for intact liver tissues (a, b) and tissues undergone plasma treatment (c, d).

As we can see in figure, the spectra of the absorption coefficient $\mu_a(\lambda)$ are inversely symmetrical to a high extent with the spectra of the reflection coefficient, however, unlike the $R_d(\lambda)$, they demonstrate a series of additional components. Comparison of the obtained results with the known literature data [21,24] show that within visible region of spectrum the coefficient $\mu_a(\lambda)$ is formed by a complex of endogenic chromophores, which includes oxy- and deoxyhemoglobin with the absorption stripes at the wavelengths 280 ± 5, 350 ± 5, 418 ± 5, 545 ± 5 and 577 ± 5 nm. Spectral component near to the wavelengths 650 ± 5 nm, apparently, is caused by absorption of porphyrine groups. Along with that, the presence of spectral components within the near infrared range is caused by the presence of lipid complexes and water in biological tissues with absorption in the region 760 ± 5, 980 ± 5, 1185 ± 5, 1450 ± 5 nm. The absorption maximum corresponds to the wavelengths 420 ± 3 nm (Soret band)

and 1450 ± 10.0 nm, where $\mu_a(\lambda)$ is reaching the values of 3.4 ± 0.4 and 2.25 ± 0.1 mm^{-1}, accordingly. Closer to the transparency window, the absorption coefficient is monotonically reducing, and within the spectral segment of $700-900$ nm is decreased up to 100 times. At that, interaction of plasma radiation with biological tissues leads to insignificant changes of the absorption coefficient (within the limits of 10%) mainly in UV and visible region of the spectrum with attenuation of the endogenic porphyrines absorption stripe, as well as to decrease of the values $\mu_a(\lambda)$ down to 20% at the wavelengths of water molecules absorption.

The most remarkable differences in the spectra of the coefficient of absorption of the studied biological tissues are shown in Fig. 6. Determination of the differentiated spectrum of absorption as

$$\delta(\lambda) = \left(\frac{\mu_a(\lambda)_{\text{Intact tissues}}}{\mu_a(\lambda)_{\text{CAP treated tissues}}} - 1 \right) \times 100\%$$

Quantitative characteristics of the content of endogenic chromophores describing the dynamics of physiological properties for liver tissues under the effect of low temperature plasma

Physiological parameters	Intact biological tissue	Biological tissues under plasma treatment
V_B — volume ratio of blood, %	9.3 ± 0.4	9.0 ± 0.4
α — degree of oxygenation of biological tissue, %	84.5 ± 2.0	89.2 ± 2.0
V_W — volume ratio of water, %	72.0 ± 2.0	62.5 ± 2.0
V_{Br} — volume ratio of bilirubin, %	2.1 ± 0.2	1.9 ± 0.2
V_L — volume ratio of lipids, %	4.2 ± 0.4	3.8 ± 0.4
A_{Mie}/B_{Mie}	87.9/0.71	181.2/0.74
A_{Ray}/B_{Ray}	$5.16 \cdot 10^{10}/4$	$1.25 \cdot 10^{11}/4$
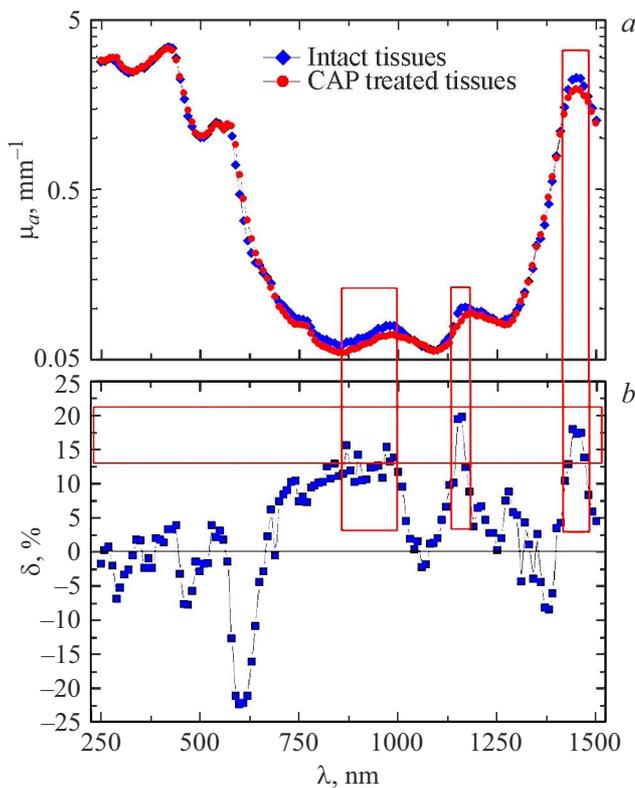
Figure 6. (*a*) Spectra of coefficient of optical absorption for intact tissues of liver and for biological tissues treated with cold plasma for 7 min. (*b*) Differential spectrum of the absorption coefficient of intact and irradiated biological tissues; three spectral intervals are distinguished, where absorption coefficients have the maximum ($\delta > 10\%$) differences: $860-1000$, $1130-1200$ and $1430-1470$ nm.

allowed to distinguish three spectral intervals that correspond to the water absorption stripes near to the wavelengths 980 ± 5, 1185 ± 5 and 1450 ± 5 nm, for which the spread value in the absorption intensity is $15-20\%$. The spectrum region at 1450 ± 5 nm is of the highest interest, where the absorption coefficient for intact samples of biological tissues is $\mu_a(1450) = 2.25\,\text{mm}^{-1}$, and for those treated with plasma — $\mu_a(1450) = 1.9\,\text{mm}^{-1}$. Absorption at the wavelengths 980 ± 5 and 1197 ± 5 nm is much weaker (0.08 ± 0.01 and $0.1\pm0.01\,\text{mm}-1$, accordingly), in addition to water, these regions can be overlapped by the absorption stripes of other chromophores, e.g. lipids that are present in liver tissues with the concentration of up to 6%, etc. All of this, apparently, is the reason for displacement of the maxima in the spectra $\mu_a(\lambda)$ of biological tissues from $970\rightarrow980$ and from $1197\rightarrow1185$ nm. At the same time, comparison of the water absorption spectrum [24] with the data of the absorption coefficient leads to the following values of the volume ratio of water and lipids for intact biological objects: $V_W = 72\%$ and $V_L = 4.5\%$, and for irradiated ones: $V_W = 62.5\%$ and $V_L = 3.8\%$ (Table).

In comparison with the absorption coefficient, the spectral contour of the coefficient of transport dissipation $\mu_s'(\lambda)$ is a smooth curve descending towards high wavelengths with the spectral minima within the region of stripes of intensive absorption of hemoglobin and water. This fact could be caused both by the growth of heterogeneity of imaginary component of the complex refraction index of the medium near to high absorption stripes, and by the rise of absorption in the region of high dissipation, when, due to increase of the number of interactions with endogenic chromophores per the length of free run, the number of multiple dissipation photons is falling [35,36].

Analysis of spectral dependence of the dissipation anisotropy coefficient by approximation thereof in the expression (4) allowed to forecast with a good accuracy $\mu_s'(\lambda)$ by the function, which for intact biological tissues looks like

$$\mu_s'(\lambda)\_\text{Calc} = 87.9\lambda^{-0.71} + 5.16 \cdot 10^{10}\lambda^{-4},$$

where the first term of sum of the function with the wave exponent $B_M \sim 0.71$ corresponds to the light dissipation

caused by large histostructures of liver (nuclei and membranes of hepatocytes, connective tissue fibrages, etc.). The second term of sum with the exponent $B_R \sim 4$ corresponds to small (Rayleigh) particles, e.g., mitochondria, lysosomes, and other elements of cytoplasm of hepatocytes, as well as individual collagen fibers of stroma and supramolecular complexes. Wherein, according to the obtained expression, main contribution into formation of the coefficient of transport dissipation is made by Rayleigh particles, whose role in the short wavelength region of the spectrum $\mu'_s(\lambda)$ is predominating, and their concentration many times exceeds that of coarse particles. It is confirmed by histological aspect of liver, according to which, mitochondria occupy more than 25% of the total volume of hepatocytes (at the average, 33 mitochondria per μm^2) [37], and there is a good concordance with the data of the works [38,39].

With regard to intact biological tissues, the processes of plasma treatment result in double growth of the coefficient of transport dissipation with increase of the inclination angle of spectral curve (Fig. 5, c), for which the approximating function looks like:

$$\mu'_s(\lambda)\_\text{Calc} = 181.2\lambda^{-0.74} + 1.25 \cdot 10^{11}\lambda^{-4}.$$

According to the obtained expressions, it means that with insignificant decrease of efficient dimensions of dissipating particles, there is 2.5 times increase of their concentration.

The use of the procedure $(1)-(4)$ allowed to evaluate the dynamics of some physiological and morphofunctional characteristics of the studied biological objects (Table) based on the value and form of spectral dependence of the coefficients $\mu_a(\lambda)$ and $\mu'_s(\lambda)$. In particular, in addition to the dynamics of morphofunctional characteristics, the effect of plasma radiation with duration of up to 7 min causes decrease of the content of water V_W, lipids V_L and bilirubin V_{Br} down to 20%, as well as increase of the value of oxygenation α up to 10% at virtually the same values of the degree of blood filling of biological tissues.

The detected physiological changes in tissues of liver could indicate the development of primary signs of dehydration. Apparently, changes in concentrations of endogenic chromophores, as well as inversible faults of histostructure of hepatocytes and architectonics of liver parenchyma are caused not only by denaturation of structural proteins and hemoglobin, but more likely by the development of the processes of compensatory dehydration of cellular ultrastructures, cells and the tissues themselves. Subject to the results of fluorescent analysis, it can be assumed that this leads to inhibition of metabolic activity of mitochondria by suppression of electrons transfer via the respiratory chain, which, as well known, is the reason for the growth of oxygen content and, consequently, increase of NADH concentration. At the same time, one of the oxygen cumulation effect is inhibition of generation of free radicals, which is manifested as decrease of the content of products of free radical oxidation of macromolecules of lipid and porphyrine complexes [29,40].

Finally, we should note that, regardless of an indirect analysis of bio-, physical and chemical effects, the results of the performed studies are in a good correlation, mutually complementary and allow to evaluate in the format *in situ* a series of the most important functional characteristics of interaction of low-temperature plasma with biological objects. However, more profound study of these processes requires performance of additional studies, both spectroscopic, and microscopic ones. In particular, it is necessary to identify the mechanisms of effect of light dissipation and reabsorption for the formation of true spectra of fluorescence, as well as to identify the specifics of activity of cold plasma in terms of histomorphological and histochemical characteristics of biological tissues. Detailed attention to these studies will be paid in next publications.

4. Conclusion

Thus, summarizing the results of the study of the effect of plasma radiation for spectral optical properties of biological tissues, we may outline the following.

1. The spectra of fluorescence $F(\lambda)$ of the studied biological tissues are formed by illumination of coenzymes of dehydrogenase NADH and FAD+, vitamin A, as well as lipids and the complex of endogenic porphyrines, at whose emission wavelengths (475±3, 510±5, 531±2, 593±5 and 635±2 nm) there are extrema.

Activity of cold plasma leads both to increase of the total level of fluorescence intensity up to 1.5 times, and to the change of the form of spectral contours of the spectra $F(\lambda)$. In particular, there is intensification of fluorescence of NAD(P)H and vitamin A — up to 30% with attenuation of illumination of lipofuscin and porphyrine complexes by 25%. This fact is manifested in the dynamics of spectral indices in the form of decrease of the indices of respiratory activity (κ_1), degradation of intracellular organs (κ_3) and hemaproteins (κ_4) up to 30% and the increase of index of antioxidant protection (κ_2) by $15-20\%$.

2. The spectra of the coefficient of diffusion reflection $R_d(\lambda)$ of liver tissues are formed by spectral stripes of absorption of oxy- and deoxyhemoglobin (280±5, 350±5, 418±5, 545±5 and 577±5 nm), as well as lipid complexes and water (760±5, 980±5, 1185±5, 1450±5 nm), near to whose wavelengths the absorption coefficient $\mu_a(\lambda)$ makes specific maxima.

3. The activity of plasma radiation leads to the growth of the coefficient of diffusion reflection up to 2 times due to increase of the coefficient of transport dissipation $\mu'_s(\lambda)$ up to 2 times, which is caused by insignificant decrease of efficient dimensions of dissipating particles and increase of their concentration up to 2.5 times. At the same time, for the absorption coefficient, these changes are associated with the decrease of the content of water, lipids and bilirubin down to 20%, as well as with the growth of the oxygenation value up to 10% at the same values of the degree of blood filling of biological tissues.

4. Analysis of the results of spectral and optical studies indicates a positive therapeutic effect of low-temperature plasma through amplification of antioxidant protection and development of the processes of compensatory dehydration.

Funding

Conflict of interest

The authors declare that they have no conflict of interest.

References

[1] A. Stancampiano, D. Forgione, E. Simoncelli, R. Laurita, R. Tonini, M. Gherardi, V. Colombo. J. Adhesive Dentistry, **21** (3), 229 (2019).

[2] A. Mariachiara, A. Venturuzzo, A. Gelmetti, E. Guasco, S. Bassissi, M. Rossi, P. Calzavara-Pinton. Clinical Plasma Medicine, **19−20**, 100110 (2020). DOI: 10.1016/j.cpme.2020.100110

[3] Th. Bernhardt, M. Semmler, M. Schäfer, S. Bekeschus, S. Emmert, L. Boeckmann. Oxidative Medicine and Cellular Longevity, **2019**, 3873928 (2019). DOI: 10.1155/2019/3873928

[4] E.A. Golubitskaya, O.S. Troitskaya, E.V. Yelak, P.P. Gugin, V.A. Richter, I.V. Schweigert, D.E. Zakrevsky, O.A. Koval. Acta Natura, **11** (3), 16 (2019).

[5] E. Sysolyatina, M. Vasiliev, M. Kurnaeva, I. Kornienko, O. Petrov, V. Fortov, A. Gintsburg, E. Petersen, S. Ermolaeva. J. Phys. D., **49**, 294002 (2016).

[6] N.Y. Babaeva, G.V. Naidis. Trends in Biotechnology, **36** (6), 603 (2018).

[7] K. Kletschkus, N. Gelbrich, M. Burchardt, A. Kramer, S. Bekeschus, M. Stope. Health Physics, **119** (1), 153 (2020).

[8] D. Xu, Q. Cui, Y. Xu, Zh. Liu, Z. Chen, W. Xia, H. Zhang, D. Liu, H. Chen, M. Kong. AIP Advances, **8** (10), 105219-1 (2018). DOI: 10.1063/1.5046353

[9] I. Trizio, E. Sardella, V. Rizzi, G. Dilecce, P. Cosma, M. Schmidt, T. Woedtke, R. Gristina, P. Favia. Plasma Medicine, **6** (1), 13 (2016).

[10] X. Sua, Y. Tianb, H. Zhoua, Y. Lib, Zh. Zhanga, B. Jianga, B. Yanga, J. Zhang, J. Fang. Appl. Environ. Microbiol., **84** (9), e02836-17 (2018). DOI: 10.1128/AEM.02836-17

[11] F. Saadati, H. Mahdikia, H.-A. Abbaszadeh, M.-A. Abdollahifar, M. Khoramgah, B. Shokri. Scientific Reports, **8** (1), 7689 (2018). DOI: 10.1038/s41598-018-25990-9

[12] A. Akbiyik, D. Sari, U.K. Ercan, Y. Uyanikgil, H. Tasli, C. Tomruk, Y.H. Usta. J. Appl. Microbiol., **131** (2), 973 (2020).

[13] K.V. Pozhar, M.O. Mikhailov, E.A. Polyakova, E.L. Litinskaia, Yu.E. Abolemova. Biomedical Engineering, **55** (2), 84 (2021).

[14] V.D. Genin, A.B. Bucharskaya, E.A. Genina, G.S. Terentyuk, N.G. Khlebtsov, V.V. Tuchin, A.N. Bashkatov. In: *Proc. of SPIE, Saratov Fall Meeting 2020: Optical and Nanotechnologies for Biology and Medicine* (SPIE, USA, 2020), Vol. 118450. DOI: 10.1117/12.2590422

[15] X. He, D. Hu, X. Fu, X. Rao. Postharvest Biol. Technol., **179**, 111570 (2021). DOI: 10.1016/j.postharvbio.2021.111570

[16] V.V. Tuchin, J. Popp, V. Zakharov. *Multimodal Optical Diagnostics of Cancer*. (Springer Nature Switzerland AG, Switzerland, 2020). DOI: 10.1007/978-3-030-44594-2

[17] J.H. Lam, K.J. Tu, S. Kim. Biomed. Opt. Expr., **12** (6), 3091 (2021).

[18] F. Ghasemi, P. Parvin, N. Sadat, H. Motlagh, S. Abachi. Biomed. Opt. Expr., **8** (2), 512 (2017).

[19] E. Tsibulskaya, N. Maslov. J. Chemometrics, **35** (6), e3343 (2021).

[20] A.A. Moghaddam, B. Sajad, F.M. Nia, S.H. Madani. J. Lasers Med. Sci., **12**, e10 (2021). DOI: 10.34172/jlms.2021.10

[21] S.L. Jacques. Phys. Med. Biol., **58** (11), 37 (2013).

[22] A.J. Welch, M.J.C. Van Gemert. *Optical-Thermal Response of Laser Irradiation Tissues*, 2nd ed. (Springer Science+Business Media, Luxembourg, 2011). DOI: 10.1007/978-90-481-8831-4

[23] V.V. Tuchin. *Optika biologicheskikh tkanei. Metody rasseyaniya sveta v meditsinskoy diagnostike*, 2nd issue (Fizmatlit, M., 2013) (in Russian).

[24] S.A. Prahl. *PhotochemCAD* [Electronic source]. URL: http://omlc.ogi.edu/spectra/PhotochemCAD/html/index.html

[25] B. Bandi. *Metody optimizatsii*, ed. by V.A. Volynsky. (Radio i svyaz, M., 1988) (in Russian).

[26] K.M. Giraev, K.S. Bekshokov. N.A. Ashurbekov, N.M. Abdullaeva, E.Kh. Israpov. Opt. Spectr., **122** (4), 632 (2017).

[27] J.R. Lakowicz. *Principles of Fluorescence Spectroscopy*, 3rd ed. (Springer Science+Business Media, Luxembourg, 2006). DOI: 10.1007/978-0-387-46312-4

[28] A.C. Croce, A. Ferrigno, G. Bottiroli, M. Vairetti. Liver International, **38**, 1160 (2018).

[29] D. Nelson, M. Cox. *Lehninger Principles of Biochemistry*. (Laboratoriya znanij, M., 2020), Volume 2.

[30] G.T. Hanson, R. Aggeler, D. Oglesbee. J. Biol. Chem., **279**, 13044 (2004).

[31] I.E. Hassinen. J. Innovative Optical Health Sci., **7**, 1350058-6 (2014).

[32] R. Carmona, S. Barrena, R. Muñoz-Chápuli. J. Dev. Biol., **7** (2), 10 (2019).

[33] A. Höhn, T. Grune. Redox Biology, **1**, 140 (2013). DOI: doi.org/10.1016/j.redox.2013.01.006

[34] S. Bayati, R. Yazdanparast. Iran Biomed J., **15** (4), 134 (2011).

[35] A.N. Bashkatov, E.A. Genina, M.D. Kozintseva, V.I. Kocubei, S.Yu. Gorodkov, V.V. Tuchin. Opt. i spektr., **120** (1), 6 (2016) (in Russian).

[36] A.N. Bashkatov, E.A. Genina, V. Kochubei. Kvant. elektron., **44**, 779 (2014) (in Russian).

[37] O.D. Myadelets. *Gistologiya, tsitologiya i embriologiya cheloveka*. (VGMU, Vitebsk, 2016) (in Russian).

[38] B. Beauvoit, M. Kimura, B. Chance. Biophys. J., **67**, 2501 (1994).

[39] J.M. Schmitt, G. Kumar. Appl. Opt., **37**, 2788 (1998).

[40] B. Halliwell, J.M.C. Gutteridge. *Free Radicals in Biology and Medicine*. (Oxford University Press, Great Britain, 2015). DOI:10.1093/acprof:oso/9780198717478.001.0001